Parker, M., Harbord, E., Young, A., Androvitsaneas, P., Rarity, J., & Oulton, R. (2018). Tamm plasmons for efficient interaction of telecom wavelength photons and quantum dots. *IET Optoelectronics*, *12*(1), 11-14. https://doi.org/10.1049/iet-opt.2017.0076

Submission Template for IET Research Journal Papers

Tamm plasmons for efficient interaction of telecom wavelength photons and quantum dots

Matthew Parker[1]*, Edmund Harbord[1,2], Andrew Young[2], Petros Androvitsaneas[2], John Rarity[2], Ruth Oulton[1,2]

[1]School of Physics, H H Wills Physics Laboratory, University of Bristol, Tyndall Avenue, Bristol, BS8 1TL
[2]Department of Electrical and Electronic Engineering, University of Bristol, Merchant Ventures Building, Woodland Road, Bristol, BS8 1UK
*mp14931@bristol.ac.uk

Abstract: We present here designs for tuneable confined Tamm plasmons (CTPs) resonant at 1.3 μm, consisting of an AlAs/GaAs distributed Bragg mirror (DBR) and gold disk. Using numerical methods we explored the effect of disk diameter on the CTP resonance and position of a dipole source (modelling a quantum dot) on emission through the disk. We found decreasing disk diameter resulted in a blue-shifted fundamental mode and that a dipole positioned in the center of the disk emitted with an angular distribution that collected 90% of the transmitted power within an NA of 0.7. We also explore the Purcell enhancement under the CTP as a function of dipole position.

1. Introduction

Semiconductor quantum dots (QDs) are an attractive solid-state source of single photons and other quantum states, such as entangled photons. Such a source would be useful for several potential technologies, such as below-shot noise measurements [1], quantum computing [2] and quantum communication [3]. The latter requires long-distance transmission of the photons while minimizing their loss or decoherence [4], [5]. It would therefore be particularly valuable to have sources that emit at wavelengths in the telecommunication bands (1.3 or 1.55 μm), as these have notably lower levels of attenuation through optical fibres. It is possible to fabricate QDs in a GaAs spacer layer, either as high-density ensembles for room temperature operation or as single-emitters at low temperature, that emit at 1.3 μm wavelengths [6], [7]. Another challenge is that QDs emit isotropically and are incorporated in high refractive index materials, which makes efficient photon extraction difficult [8].

Tamm Plasmons (TPs) are a type of optical surface mode, first proposed by Kaliteevski, et al. [9], that exist between a metal layer and a dielectric Bragg reflector (DBR) (figure 1(a)). The light is confined by the metal's negative dielectric constant and by the photonic bandgap of the DBR. The top layer of the dielectric, labelled the spacer layer, must have the higher of the two refractive indices of the DBR [10]. The interaction between these modes and QD emitters compares favourably to other surface-confined optical modes, such as surface plasmon polaritons: the majority of the mode is located within the lossless, photonic material; they have a parabolic dispersion that is within the light cone, so can be excited without requiring momentum-matching components which complicate miniaturization [11]; and they can be excited with both TE and TM polarized light. Finally, lateral confinement can be added by limiting the lateral dimensions of the metallic layer to make confined Tamm Plasmons (CTPs) [12].

Increasing confinement results in a blue shift of the fundamental mode resonance [12], [13]. CTPs with asymmetric metal shapes can excite non-degenerate modes at different polarizations [14]. Hence, the wavelength and polarization resonance can be shaped using simple metal deposition techniques. This avoids the need to etch the QD-containing layers, which is thought to lead to charge noise in the structure [15], [16]. CTPs have already been demonstrated in several QD-based applications such as lasers [17] and single-photon sources [18], [19] but to our knowledge have never been considered in the telecoms wavelength regime. In addition, the relation between the QD's position relative to the mode and how this affect its emission characteristics, such as lifetime and emission angle, is complex and poorly understood.

In this we paper we design CTPs resonant at 1.3 μm, using Transfer Matrix Method (TMM) calculations together with a commercial finite-difference time domain (FDTD) solver [20]. We also explore the effect of varying confinement (disk diameter) and source position.

2. Results of Transfer Matrix Method (TMM) calculations

One dimensional TPs (i.e. with no lateral confinement) are first studied using the Transfer Matrix Method (TMM) [21] consisting of 17.5x λ/4 DBR pairs of GaAs and AlAs, a GaAs spacer layer and a gold (Au) metal layer. While silver is often used for Tamm plasmon structures, gold offers greater resistance to tarnishing. Refractive index values were taken from the literature [22]–[24]. The metal and spacer thickness for 1.3 μm resonance was found at 25 nm and 75 nm. Figure 1(b) shows the reflectivity spectra for the bare DBR (blue line) is shown with a high reflectivity photonic stopband present between 1205 nm and 1375 nm. Adding the metallic

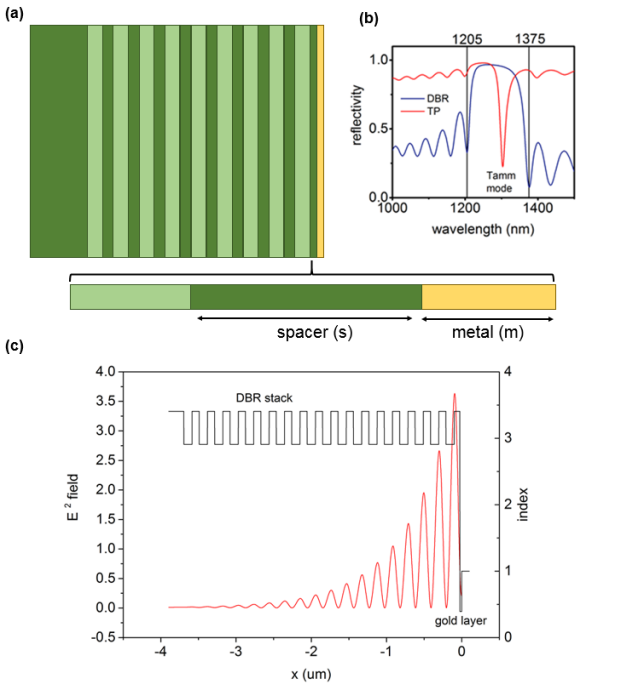

Fig 1. (a)*; diagram of the Tamm Plasmon structure.* ***(b)****; reflectivity spectrum at normal incidence on a planar Tamm structure with 17.5x DBR pairs (AlAs/GaAs) with respective thicknesses 110/95 nm, spacer (GaAs) layer thickness of 75 nm and Au layer thickness of 25 nm, shown with (red) and without (blue) metal layer. Black lines show the first minima of the DBR stopband.* ***(c)****; profile of refractive index (black) and electrical field intensity at λ = 1300 nm (red) for the structure described above. Both the field profile and reflectivity are calculated using the TMM.*

layer (red line) shows the appearance of the TP as a dip in the reflectivity at λ_{TP} = 1304 nm. This occurs due to light at wavelengths close to the resonance coupling into the TP mode and being guided into the spacer layer, instead of being reflected. Figure 1(c) shows both the profile of the calculated electric field intensity (red) as well as refractive index (black) through a cross-section of the structure. The enhancement of the electric field intensity in the spacer layer is clearly visible, as well as the decay deeper into the structure.

The mode's resonance wavelength dependence on the metal and spacer layer thicknesses are shown in figure 2(a) and 2(b) respectively, and the mode's quality factor (Q factor) dependence on metal and spacer layer thickness in figure 2(c) and 2(d). Our structure results in a TP with a Q-factor of just under 70. Increasing the Au thickness results in an increased Q, which is consistent with other results [25], but also results in reduced transmission through the structure due to absorptive losses in the metal (not shown). Variation of the spacer layer has little effect on the Q-factor. In contrast, the shift in the mode resonance is small for variations in the Au layer and large for the spacer layer; by changing the spacer thickness from 40 nm to 100 nm the TP mode can effectively cover nearly the full range of the O-band (1260 nm to 1360 nm) without significant variation of quality factor.

3. Results of FDTD simulations

In this section we analyse the results of FDTD simulations of fully confined Tamm Plasmons. Our structure consists of 17.5 x λ/4 DBR pairs of GaAs and AlAs, a 75 nm GaAs spacer layer and a 25 nm Au disk with diameter *d* (figure 3(b) inset). We explore the effect of confinement (disk diameter) and effect of source position with respect to the disk on the emission properties.

3.1 Effect of disk diameter

Reducing the diameter of the Au disk causes an increasing confinement of the CTP. Figure 3(a) shows the resonant frequencies under the disk as the diameter is changed. A transverse electric (TE) dipole source was positioned in the middle of the spacer layer at the center of the Au disk and emitted over the spectral range 1100 nm to 1400 nm (pulse length = 8 fs). The resonances of the structure were found by taking the Fourier transform of the electric field at several points in the spacer layer and for the duration of the simulation. An initial cut-off of 200 fs was used and the fields were observed to fully decay during the runtime for all diameters.

As the disk diameter is reduced there is a disappearance of higher order modes until only the lowest energy, fundamental mode remains, this effect becoming predominant once the disk is below a diameter of 4 μm. As the disk size is further reduced there is a shift in the resonance peak to higher energies. However as the mode becomes more confined there is also a corresponding decrease in quality factor, as shown by the change in peak widths in 3(a), believed to be due to coupling to scattered modes at the edge of the disk [12].

Figure 3(b) further shows the identified fundamental mode energies for a range of disk diameters. The rapid

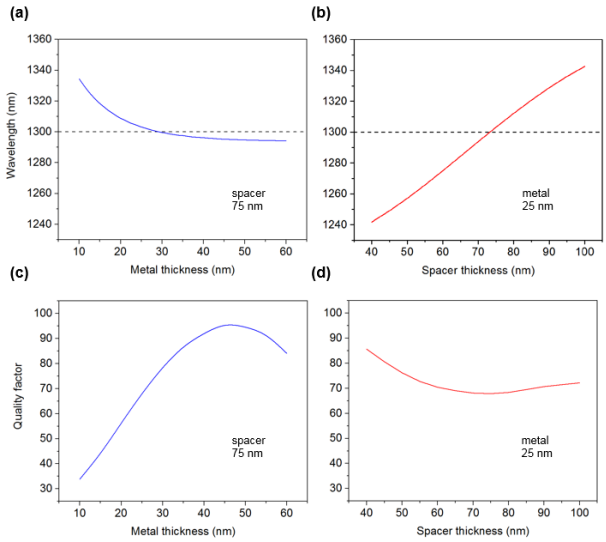

Fig 2. (a) *and* ***(b)****; calculated shift of resonance position of the TP as a function of Au and spacer layer thickness respectively. Structure consists of 17.5x AlAs/GaAs pair DBR and the spacer and metal thicknesses are respectively kept constant at 75 nm and 25 nm.* ***(c)*** *and* ***(d)****; shift in quality factor as a function of Au and spacer layer thickness respectively.*

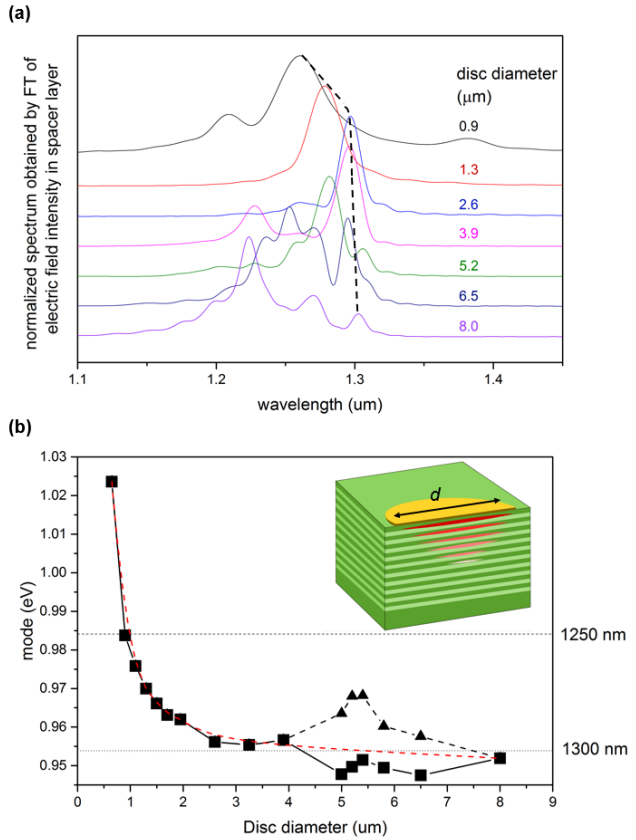

Fig 3. (a)*; resonant frequencies for confined Tamm Plasmons as a function of disk diameter and guide to the fundamental mode (dashed line). Calculated with FDTD method as described in text.* ***(b)****; identification of the fundamental modes of the CTP at different diameters. Au layer thickness is 25 nm and spacer thickness is 75 nm. Overlapping with higher order modes, particularly between 5 to 7 μm, result in more than one possible mode to be identified. Therefore, square and triangle symbols show the two lowest energy modes identified for disk diameters between 5 and 7 μm. The dashed red line is an exponential fit to only the data points outside these diameters.* ***Inset****: diagram of the confined Tamm Plasmon (CTP)*

blueshift of the CTP resonance can be readily seen as the mode is confined by the smallest diameter disks. For larger disks the structure come to resemble the fully planar structure and the resonance was found to asymptotically tend to the 2D case (calculated using TMM) where there are no confinement effects. We compare the spectra of the 2.6 μm (blue) and 8.0 μm (violet) diameter disks in 3(a): the former has a single peak at 1294 nm, a slight blue shift from the planar TP; while the 8.0 μm disk has at least three identifiable resonances. The lowest energy peak, at 1303 nm, is identical to that for the TMM as expected.

In contrast, the spectra for diameters between 4 μm and 8 μm is less clear. It is possible to identify multiple modes that overlap around 1290 to 1310 nm, which is inconsistent with the trend towards high energies at lower diameters and the TMM energy at large diameters. Two possible interpretations of the fundamental resonances are shown in 3(b) as squares (lowest energy) and triangles (highest energy). Future work will focus on elucidating the complex mode structure associated with the CTP.

3.2 Effect of source position

We next considered the effect on emission when the dipole was displaced from the center of the disk. An Au disk with a diameter of 2.6 μm was excited by a TE dipole source at the center of the fundamental mode (1296 nm), which was moved in the *y*-direction (origin at $y = 0$; edge of disk at $y = 1.3$ μm) (figure 4(a)). This diameter was chosen as it maximized the amount of emission collected through the top of the structure.

The electric near field was recorded above the disk and reduced to a set of plane waves, which are projected into the far field using Lumerical's far field solver to find the angular distribution of transmitted light. Figure 4(b) shows a slice through the far field for a fixed radius and ϕ angle (that is, the dashed line in 4(a)). For a dipole positioned in the center the angular distribution of the emission has a Gaussian profile (black dashed line) centered on θ = 0 with a width of 57.4 ± 0.9°. This compares to a width of 106.5 ± 2.4° for the structure with no metal layer (orange line). As the source moves towards the edge of the disk there is a shift in the emission peak to higher angles and to a wider distribution. As the dipole is shifted from the center position it couples less into the fundamental mode, which has a transverse profile with maximum field enhancement in the center of the disk. The far field emission instead becomes a mixture of Gaussian and increasingly non-Gaussian radiative patterns. There is also a large drop in field intensity as less light is transmitted through the top of the structure. We suggest this is a combination of increased losses into the side channel and scattering at the edge of the disk.

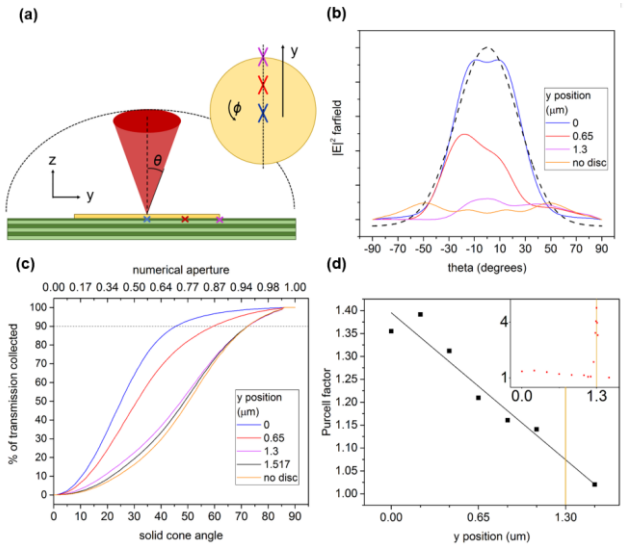

Fig 4. (a)*; diagram of dipole position under metal disk.* ***(b)****; simulation of the projected far field emission at the fundamental resonance for* d *= 2.6 μm (λ = 1296 nm), showing the profile for a fixed ϕ angle as the source is moved away from the disk center. The black line shows the Gaussian fit for y = 0 (blue) projection.* ***(c)****; percentage of power in the far field collected in a cone with solid half-angle θ (i.e. the angle to the cone axis) over all transmitted power through the top of the structure.* ***(d)****; shift in Purcell factor as a function of source displacement.* ***Inset:*** *Including Purcell factors as source approaches the disk edge and plasmonic effects occur.*

The increased angular distribution is further demonstrated in figure 4(c) which plots the far field power integrated across a spherical surface element between [θ, -θ] and given as a percentage of all transmitted power in the far field (i.e. through the whole hemisphere). For the whole cavity mode 70% of the power is emitted through the top channel, though the largest loss is still into the side channel. For a dipole under the center of the disk 90% of power transmitted through the top of the structure occurs within a cone with an equivalent numerical aperture (NA = n sinθ) of 0.7. Low-loss objectives of this NA are commercially available, and are used in telecom wavelength spectroscopy of single quantum dots. This implies that Tamm plasmons are promising photonic structures for collection of single photons at this wavelength. The NA increases as the dipole moves towards the edge of the disk until the limit of a dipole outside the disk region entirely, which has a NA = 0.95. The emitted power distribution was identical to a dipole with DBR but no disk (orange line). The loss of directivity once the dipole is more than half of a radius from the disk center has the benefit of spatially selecting the QDs that would have emission collected by a low NA objective.

In addition to directionality of emission the CTP is also expected to change the emission rate of a QD though Purcell enhancement. Figure 4(d) shows the Purcell factor decreases linearly as a function of distance to the disk center. However, this trend breaks down in the region very close to the disk edge (figure 4(d) inset), where there is a very large enhancement in the Purcell factor. The precise cause of this is uncertain but we propose this is caused by the excitation of surface plasmons at the metal-air interface. This would explain the narrowness of the region around the edge where this enhancement occurs as resulting from a tightly confined, evanescent mode.

4. Conclusion

In conclusion, we have designed CTP structures that are resonant at 1.3 μm and have demonstrated it is possible to control the resonance through changing the spacer layer thickness or disk diameter across the range of the O-band. We have also explored the effect of dipole position on the emission from these modes and found that a centrally positioned source has both a Purcell enhancement (of around 1.4) and emits 90% of the transmitted power within a NA of 0.7. These results need to be confirmed experimentally. Further work also needs to be done on understanding the effects at the disk edge and improving overall transmission into the top channel. However, of this emission the CTP presents a device with good collection characteristics for QDs, that is easily fabricated and which is tuneable through the telecoms range.

5. Acknowledgements

This work is funded by EPSRC grant EP/M024156/1.

6. References

[1] M. Xiao, L. A. Wu, and H. J. Kimble, “Precision measurement beyond the shot-noise limit,” *Phys. Rev. Lett.*, vol. 59, no. 3, pp. 278–281, 1987.

[2] D. P. DiVincenzo and IBM, “The Physical Implementation of Quantum Computation,” *Fort. Phys.*, vol. 48, pp. 771–793, 2000.

[3] N. Gisin, G. Ribordy, W. Tittel, and H. Zbinden, “Quantum cryptography,” *Rev. Mod. Phys.*, vol. 74, no. 1, pp. 145–195, 2002.

[4] V. Scarani, H. Bechmann-Pasquinucci, N. J. Cerf, M. Dušek, N. Lütkenhaus, and M. Peev, “The security of practical quantum key distribution,” *Rev. Mod. Phys.*, vol. 81, no. 3, pp. 1301–1350, 2009.

[5] K. De Greve *et al.*, “Quantum-dot spin–photon entanglement via frequency downconversion to telecom wavelength,” *Nature*, vol. 491, no. 7424, pp. 421–425, 2012.

[6] E. Clarke *et al.*, “Persistent template effect in InAs/GaAs quantum dot bilayers,” *J. Appl. Phys.*, vol. 107, no. 11, 2010.

[7] T. Kaizu, T. Matsumura, and T. Kita, “Broadband control of emission wavelength of InAs/GaAs quantum dots by GaAs capping temperature,” *J. Appl. Phys.*, vol. 118, no. 15, pp. 1–7, 2015.

[8] W. L. Barnes *et al.*, “Solid-state single photon sources: Light collection strategies,” *Eur. Phys. J. D*, vol. 18, no. 2, pp. 197–210, 2002.

[9] M. Kaliteevski *et al.*, “Tamm plasmon-polaritons: Possible electromagnetic states at the interface of a metal and a dielectric Bragg mirror,” *Phys. Rev. B - Condens. Matter Mater. Phys.*, vol. 76, no. 16, pp. 1–5, 2007.

[10] A. R. Gubaydullin *et al.*, “Enhancement of spontaneous emission in Tamm plasmon structures,” *Sci. Rep.*, vol. 7, no. 1, p. 9014, 2017.

[11] M. E. Sasin *et al.*, “Tamm plasmon polaritons: Slow and spatially compact light,” *Appl. Phys. Lett.*, vol. 92, no. 25, pp. 1–4, 2008.

[12] O. Gazzano *et al.*, “Evidence for confined Tamm plasmon modes under metallic microdisks and application to the control of spontaneous optical emission,” *Phys. Rev. Lett.*, vol. 107, no. 24, pp. 4–8, 2011.

[13] F. Feng *et al.*, “Confined Visible Optical Tamm States,” *J. Electron. Mater.*, vol. 45, no. 5, pp. 2307–2310, 2016.

[14] G. Lheureux *et al.*, “Polarization-Controlled Confined Tamm Plasmon Lasers,” *ACS Photonics*, vol. 2, no. 7, pp. 842–848, 2015.

[15] A. V. Kuhlmann *et al.*, “Charge noise and spin noise in a semiconductor quantum device,” *Nat. Phys.*, vol. 9, no. 9, pp. 570–575, 2013.

[16] P. Androvitsaneas *et al.*, “Charged quantum dot micropillar system for deterministic light-matter interactions,” *Phys. Rev. B - Condens. Matter Mater. Phys.*, vol. 93, no. 24, pp. 1–5, 2016.

[17] C. Symonds *et al.*, “Confined Tamm Plasmon Lasers,” *Nano Lett.*, vol. 13, pp. 3179–3184, 2013.

[18] O. Gazzano *et al.*, “Single photon source using

confined Tamm plasmon modes," *Appl. Phys. Lett.*, vol. 100, no. 23, pp. 10–14, 2012.
[19] T. Braun, V. Baumann, O. Iff, S. Höfling, C. Schneider, and M. Kamp, "Enhanced single photon emission from positioned InP/GaInP quantum dots coupled to a confined Tamm-plasmon mode," *Appl. Phys. Lett.*, vol. 106, no. 4, p. 41113, 2015.
[20] "Lumerical Solutions, Inc." [Online]. Available: http://www.lumerical.com/tcad-products/fdtd/.
[21] P. Yeh, A. Yariv, and A. Y. Cho, "Optical surface waves in periodic layered media," *Appl. Phys. Lett.*, vol. 32, no. 2, pp. 104–105, 1978.
[22] P. B. Johnson and R.-W. Christy, "Optical constants of the noble metals," *Phys. Rev. B*, vol. 6, no. 12, p. 4370, 1972.
[23] R. E. Fern and A. Onton, "Refractive index of AlAs," *J. Appl. Phys.*, vol. 42, no. 9, pp. 3499–3500, 1971.
[24] T. Skauli *et al.*, "Improved dispersion relations for GaAs and applications to nonlinear optics," *J. Appl. Phys.*, vol. 94, no. 10, pp. 6447–6455, 2003.
[25] Y. Chen *et al.*, "Effect of metal film thickness on Tamm plasmon-coupled emission.," *Phys. Chem. Chem. Phys.*, vol. 16, no. 46, pp. 25523–30, 2014.